UAV Imaging of the Riverbed in Small Tree-Lined Streams: Importance of the Light Environment

Richard David Hedger * and Marie-Pierre Gosselin

Posted Date: 4 June 2025

doi: 10.20944/preprints202506.0278.v1

Keywords: UAV; riverbed; light; cloud; sunglint; shadow

 doi:10.20944/preprints202506.0278.v1

Article

UAV Imaging of the Riverbed in Small Tree-Lined Streams: Importance of the Light Environment

Richard Hedger * and Marie-Pierre Gosselin

Norwegian Institute for Nature Research - NINA , PO Box 5685 Torgarden, NO-7485 Trondheim, Norway

* Correspondence: richard.hedger@nina.no

Abstract: UAVs are an ideal platform for remote sensing of riverbeds in small, tree-lined streams, allowing unobstructed viewing of the channel at high spatial resolution. However, effective UAV surveying of these riverbeds is hindered by a range of phenomena associated with the complex light environments of rivers, and small tree-lined streams in particular, including reflections of the overlying cloud layer from the water surface, sunglint on the water surface, and shadows from topography and riparian vegetation. Using RGB UAV imagery acquired from a range of small, tree-lined streams under a range of light conditions, we identify the prevalence of the main phenomena – reflections of clouds, sunglint, and shadows – that hinder the ability to remotely sense the riverbed. We characterize how large a constraint this is on the optimal imaging window. We then examine the degree to which sub-optimal light conditions may restrict this window, both within the year and within the day, across Europe. Our investigations suggest that different regions across Europe will have different priorities with regard to imaging, with surveys in northern rivers emphasizing avoiding low irradiant intensity in winter, and those in southern rivers emphasizing avoiding sunglint around midday. We use our findings to suggest a protocol for improved riverbed imaging that is specific to the light environment of the stream under investigation.

Keywords: UAV; riverbed; light; cloud; sunglint; shadow

1. Introduction

Obtaining information on the riverbed via remote sensing is an important component of river surveying across a range of scientific disciplines, from geomorphology and hydromorphology [1,2] to freshwater ecology [3,4]. Remote sensing can be used to provide diverse, detailed information on riverbed characteristics such as sediment composition [5], aquatic vegetation [6], fish spawning sites [7,8], and the presence of animals embedded in the substrate [9]. Remote sensing is increasingly used for the monitoring and post-facto evaluation of river restoration measures, such as the responses of riverbeds to flow regime modification, removal of barriers, and the addition of bed material [10].

Remote sensing of riverbeds using passive optical imaging presents challenges due to a range of phenomena that affect the outgoing light signal from the bed. Firstly, it is necessary to have a sufficiently high solar elevation so that (1) incoming light is not reflected off the water surface as Fresnel reflectance [11,12] and (2) incoming light intensity (irradiant intensity) is high enough so that enough light penetrating the water surface can reach the riverbed to be reflected to reach the sensor. This may pose a particular problem when imaging in high latitude environments away from the summer solstice, which are dominated by low solar elevations or even polar night. A high enough solar elevation to provide sufficient irradiant intensity is only a first prerequisite. When imaging during overcast skies, imagery of the river channel may be dominated by reflections of overlying clouds from the water surface that completely mask the underlying riverbed. Cloud cover is typically >75% within Europe [13] so this may be a major constraint on when the riverbed can be effectively imaged. Conversely, when imaging under cloud-free conditions, sunglint and shadows may be present. Sunglint – specular reflection from the water surface into the sensor when the angle of

 doi:10.20944/preprints202506.0278.v1

incidence of light on the water surface is equal to the view angle – results in optical sensors becoming saturated [14,15]. Sunglint on a flat water surface will likely be evident in imagery when the solar elevation is ≤ half the field-of-view (FOV) of the sensor [16]; sunglint on a rippled surface will be evident at even lower solar elevations due to the wider range of surface angles present across the ripples. Shadows resulting from the obstruction of direct sunlight by topography and riparian vegetation [17] make riverbed detail less visible [18]. Other optical phenomena exist – for example shallow water wave lensing involves ripples focusing light speckles on the bed [19] – that may further limit the ability to discern the riverbed. The effect of phenomena that hinder imaging of the riverbed vary both spatially and temporally across a range of scales, ranging temporally from seconds to intra-annually, and spatially from centimeters to the entire length of the river. Cloud cover varies regionally and throughout the year; irradiant intensity and the prevalence of sunglint and shadow vary spatially across regions and temporally within any given day or year as a function of solar elevation and azimuth. Variation in the light environment suggests that there will be an optimal window that is specific to location for remote sensing of the riverbed.

Much of the research relating to remote sensing of rivers is conducted in moderate sized rivers (e.g. widths of 10 – 100 m) within well-defined floodplains. Smaller streams, often in upstream tributaries and often in V-shaped and tree-lined valleys pose a particular problem with respect to remote sensing. Firstly, when imaging from a platform that is not perfectly following the river channel (e.g. a fixed-wing aircraft flying several hundred meters above the ground), trees may completely obstruct line-of-site to the channel. Secondly, channel shading may be more significant. Steep topography in V-shaped valleys and tall riparian vegetation will cast shadows which may span the entire stream channel, something that is less prevalent for wider, lowland rivers. The result is that even when the riverbed is visible, it may be poorly illuminated, and little detail may be evident in riverbed imagery (see Figure 1a). Thus, the optimal imaging window is even more restricted in small, tree-lined streams. UAVs are an obvious solution to mitigating these problems. Firstly, it is possible to fly along the river channel, below the tree canopy elevation, so that the riverbed is visible from the platform (see Figure 1b). Secondly, the flexibility of controlling UAV flight parameters allows for minimizing light phenomena that hinder successful imaging (e.g. selection of a time of day when shadows do not fall over the channel). Finally, the nature of UAV imaging allows for application of post-processing methods which may expand the window when a riverbed can be successfully imaged. For example, if the light-induced patterns are ephemeral over the short-term – for example, sunglint or wave lensing caused by moving ripples – it may be possible to remove this by acquiring video data and temporally filtering the data to remove the ephemeral phenomena.

 doi:10.20944/preprints202506.0278.v1

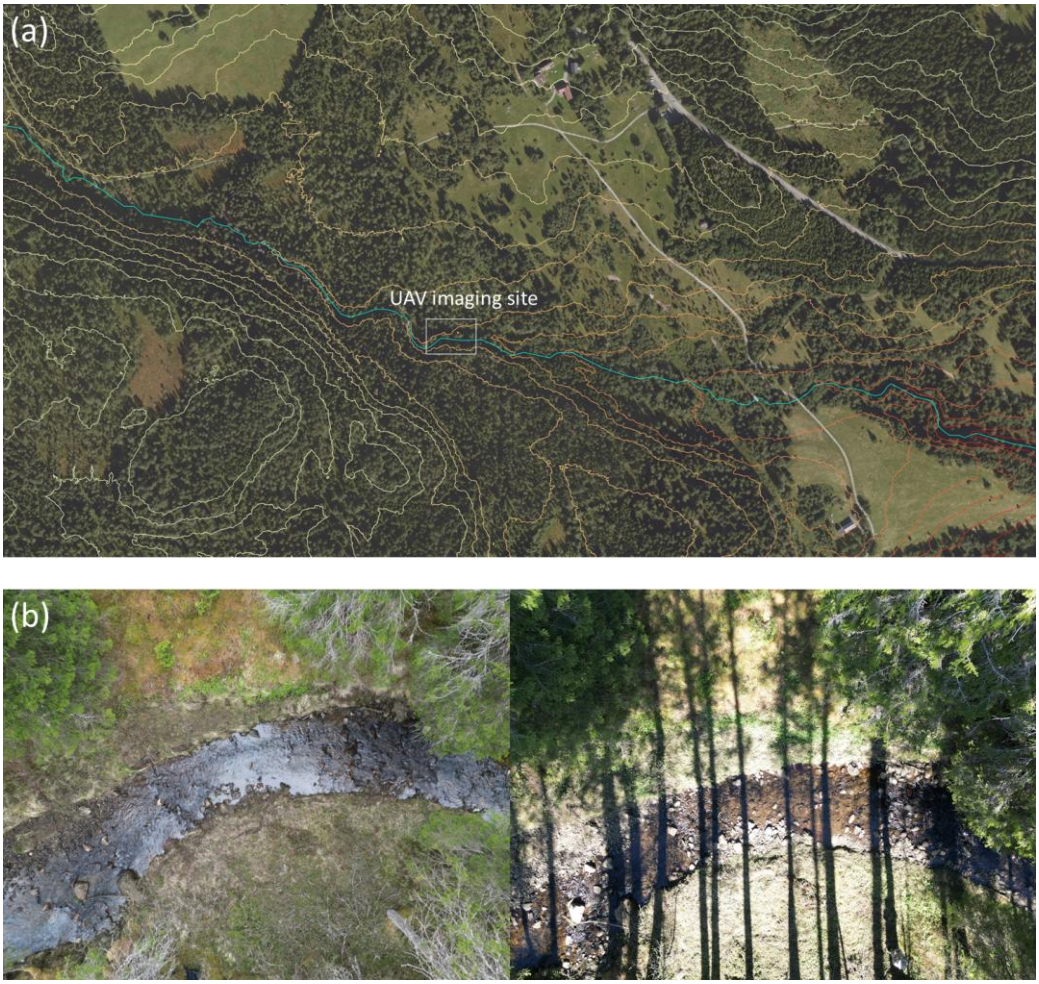

Figure 1. Example of airborne remote sensing imagery of a small, tree-lined stream (Kobberdamsbekken, Norway): (a) aerial orthophoto; (b) UAV imagery. In (a) the orthophoto (0.1 m spatial resolution) was acquired from an image archive (Norwegian Mapping Agency; www.norgeibilder.no); contours were derived airborne topographic LiDAR data (Norwegian Mapping Agency; http://hoydedata.no) (separation between contours = 20 m). In (b) two UAV images are shown: an image acquired under overcast conditions (left panel) and an image acquired under cloud-free conditions (right panel).

Here we assessed the impact of the light environment on the ability to use UAVs using light-weight RGB cameras to successfully survey the riverbed in small tree-lined streams. We firstly identified the prevalence of phenomena that hinder riverbed imaging using UAV surveys conducted as part of ongoing research programs that were acquired in small, tree-lined streams in Norway under a range of light conditions. We then identified how big a constraint on the optimal imaging window these phenomena were for the study region: that is, to provide an indication of how limited the window would be within a cloudy and high-latitude environment where streams are often obscured by topography and riparian vegetation. We then generalized our findings to determine constraints on the optimal imaging window within a larger, regional European context. Finally, we used our findings to develop a protocol for UAV surveying of small, tree-lined streams that takes the temporally variable nature of the light environment into account.

2. Materials and Methods

2.1. UAV Surveys

To assess the prevalence of light-dependent phenomena that might hinder riverbed imaging, we examined data obtained from UAV surveys (N = 26) conducted as part of ongoing research

 doi:10.20944/preprints202506.0278.v1

campaigns in six high latitude (63.38-67.20°N) streams in Central and Northern Norway – Leirelva, Kobberdamsbekken, Baklibekken, Borråselva, Akebakken, and Mølnelva (Figure 2; Table 1). This post-facto investigation of pre-existing survey data provided a range of ambient light conditions that are typically present when surveying small streams within Norway as part of river monitoring programs. Sites were surveyed under a range of light conditions (Table 1), from cloud-free to overcast skies, and from low to high solar elevation. Average irradiant intensities (estimated using the solrad library in R) ranged from <100 W m^{-2} to >600 W m^{-2}. The sites also provided a range of shading characteristics in terms of surrounding topography and riparian vegetation. For instance, the sites imaged in Borråselva and Baklibekken were surrounded by steep, tree-lined slopes and were strongly affected by shadow. The site imaged in the Leirelva, in contrast, was characterized by a flat riparian zone, with less tree cover so provided conditions that were largely shadow-free regardless of solar position. All imaged sites had sufficiently shallow depths (<1.5 m) that riverbeds were visible during direct sunlight on the water surface.

Surveys were done using the off-the-shelf micro-rotor UAV DJI Mini 2 & 3 because its small size makes it appropriate for flying over narrow, tree-lined streams below the elevation of the tree canopy. Imagery were acquired using a 1/2.3" CMOS sensor with a 12 MP camera (image dimensions = 4000 × 3000 pixels for a 4/3 aspect ratio), a fixed-aperture F2.8 lens with an 83° FOV, and an ISO range of 100-3200. Surveys varied in length but were typically short (<50 m), with the UAV flying at 5 – 10 m above the water surface which provided spatial resolutions from ca. 0.25 – 0.5 cm. Both still images and video were acquired, in all cases using auto-exposure.

 doi:10.20944/preprints202506.0278.v1

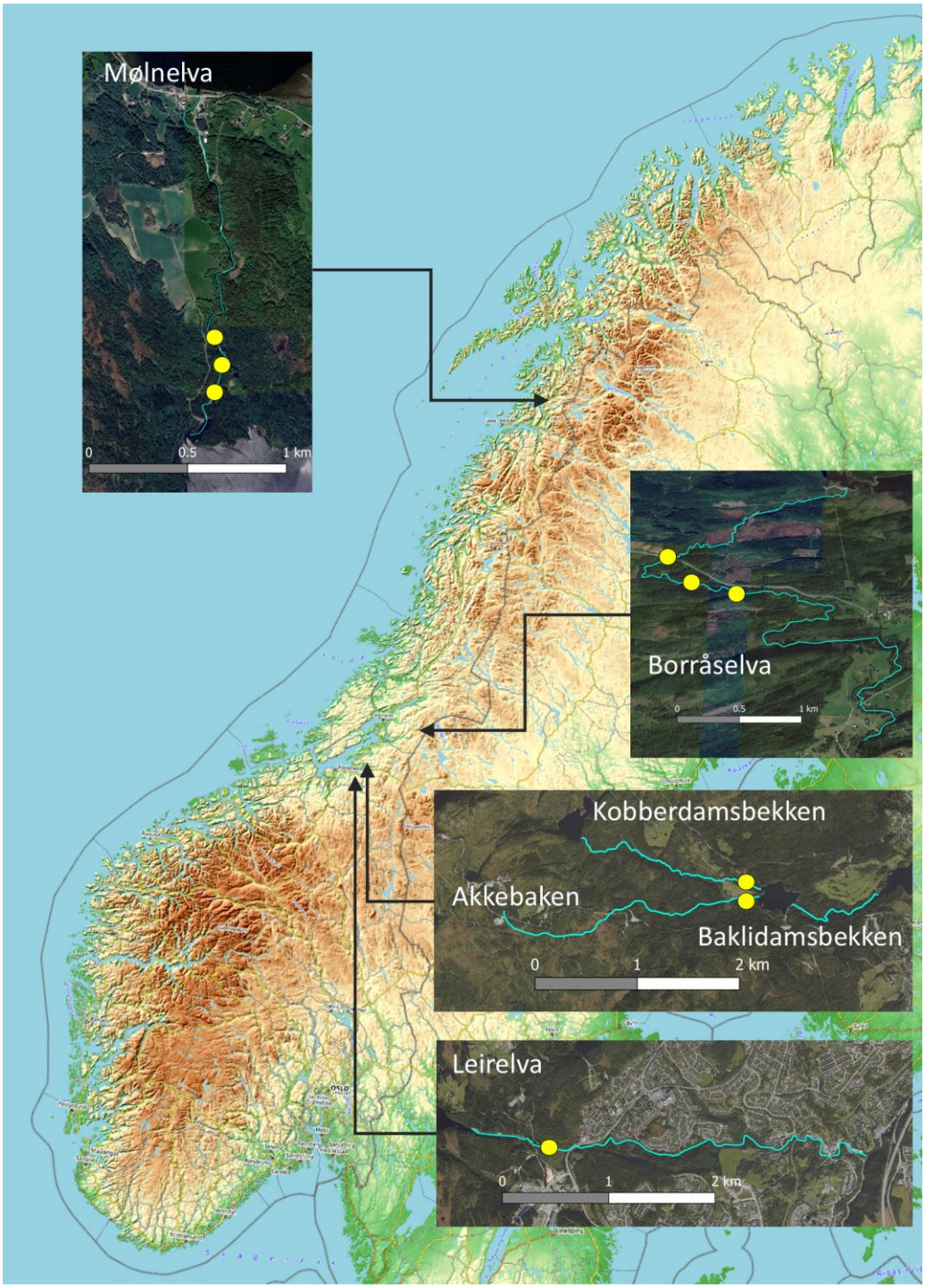

Figure 2. Study streams, showing locations of imaged sites (filled yellow circles).

Table 1. UAV surveys. Solar elevation and irradiance have been estimated for the mid-point of the survey time using the R solrad library.

River	Date	Time	Sky conditions	Solar elevation (°)	Irradiance (W m^{-2})
Leirelva	2022-04-23	12:05-12:14	Cloud-free	38.7	484
	2023-02-11	12:42-12:54	Cloud-free	11.6	70
	2023-03-09	13:31-13:36	Cloud-free	19.5	178
	2023-05-05	13:59-14:26	Cloud-free	37.1	456
Kobberdamsbekken	2022-07-19	18:34-18:35	Overcast	15.5	113

 doi:10.20944/preprints202506.0278.v1

	2022-07-25	13:23-13:30	Overcast	44.2	558
	2022-07-28	17:42-17:51	Cloud-free	19.1	164
	2022-07-30	09:16-09:33	Cloud-free	37.4	456
	2022-08-02	13:23-13:30	Cloud-free	42.3	531
	2024-05-11	11:46-12:10	Overcast	44.5	567
	2024-05-17	12:03-12:33	Cloud-free	45.8	585
Baklibekken	2022-07-11	12:32-12:39	Overcast	48.4	616
	2022-07-12	09:56-09:58	Mixed	43.4	545
Akebakken	2022-07-12	10:22-10:27	Mixed	45.3	573
	2022-08-02	14:02-14:06	Cloud-free	40.1	497
Borråselva	2022-05-31	13:53-14:13	Overcast	43.3	546
	2022-05-31	13:41-13:45	Overcast	44.7	566
	2022-05-31	13:24-13:29	Overcast	45.7	581
	2022-06-30	15:50-15:54	Cloud-free	35.1	417
	2022-06-30	14:37-15:22	Cloud-free	40.3	499
	2022-08-18	11:57-12:04	Cloud-free	39.4	490
	2022-08-18	12:21-12:24	Cloud-free	39.3	488
	2022-08-18	12:52-12:57	Cloud-free	38.6	478
Mølnelva	2022-09-29	12:07-12:24	Mixed	19.4	174
	2022-09-30	09:59-10:38	Cloud-free	17.4	144
	2022-10-01	12:03-12:14	Cloud-free	18.7	163

2.2. Light-Dependent Constraints on the Optimal Imaging Window

Light-dependent constraints on the optimal imaging window for effectively observing the riverbed were determined by (1) identifying the influence of the light environment on the ability to discern the riverbed within the collected UAV imagery, and (2) predicting the prevalence of these light environment conditions throughout the year and throughout the day. From examining the UAV imagery, we identified issues relating to (1) cloud cover, (2) solar elevation, irradiance and sunglint, and (3) solar position and shadow. We predicted these conditions as follows:

Cloud cover. Cloud cover manifested in imagery as water surface reflections that obscured the riverbed. We determined the prevalence of cloud cover at the study sites from the Cloud Fraction dataset (https://neo.gsfc.nasa.gov/view.php?datasetId=MODAL2_M_CLD_FR) of the NASA Earth Observations portal (https://neo.gsfc.nasa.gov/). This dataset is based on Aqua/MODIS satellite data and provides mean cloud cover fraction per pixel (0.1° spatial resolution) per month. Using data from 2016 – 2019, we calculated the mean cloud cover for each month at each survey site.

Solar elevation, irradiance and sunglint. Solar elevation determined irradiant intensity (W m^{-2}) and therefore the visibility of the riverbed. We calculated solar elevation and total irradiant intensity (direct + diffuse) using the solrad library in R (https://github.com/bbcrown/solrad) [20] for a latitude of 63°N (the average of the survey sites) as a function of time of year and time of day. By comparison of riverbed visibility in our UAV imagery and corresponding irradiant intensities, we were able to identify intra-annual and intra-diurnal constraints on when there would be sufficient irradiant intensity for optimal imaging. Solar elevation also determined the propensity for sunglint and Fresnel reflectance. Using information of when sunglint was present from the UAV surveys, we established an upper solar elevation threshold for avoidance of sunglint on ripples at 20°. Based on the sensor FOV, we established an upper solar elevation threshold for avoidance of sunglint on a flat surface at 40°. Very low solar elevations lead to high reflectance from the water surface (Fresnel reflectance), so we established a lower solar elevation threshold at 10°. Thus, an optimal window for avoiding sunglint and Fresnel reflectance would lie between 10 and 20° for a rippled surface and 10 and 40° for a flat surface. We then mapped these conditions as a function of time of year and time of day for the average position of the survey sites (63°N).

Solar position and shadow. To examine the prevalence of shadow on the stream channels, we predicted shadow positions for the survey sites under a range of solar elevations and azimuths. First,

 doi:10.20944/preprints202506.0278.v1

we predicted solar elevations and azimuths for two dates – June 21 (summer solstice) and September 21 (autumn equinox) for each of the streams using the solrad library. Second, we estimated shadow positions for each solar elevation and azimuth by applying a shade prediction algorithm (R function insol::doshade) to a 1 m resolution topographic LiDAR-derived Digital Surface Model (DSM) which showed the combined elevation of surrounding topography and riparian vegetation (Norwegian Mapping Agency; http://hoydedata.no). Third, the proportion of the length of each stream that was under shadow for each solar elevation and azimuth was estimated from the overlap between predicted shadow locations and the stream course as derived from a dataset on Norwegian rivers (NVE Elvenett/ELVIS; https://www.nve.no/kart/kartdata/vassdragsdata/elvenettverk-elvis/).

2.3. Regional Patterns of the Optimal Imaging Window Across Europe

Based on our findings for light-dependent constraints on optimal imaging for the survey sites, we predicted temporal and regional patterns in the optimal imaging window across Europe. We chose this region because it covers an expansive geographical area with a range of light environment conditions in terms of cloud cover, irradiance and propensity to sunglint. First, we used NASA's Cloud Fraction dataset to determine the number of cloud free days throughout Europe, year-round, and separately for summer and winter. Secondly, we determined the number of hours per day as a function of time of year and latitude where irradiance levels would be great enough to allow effective imaging of the riverbed, using >100 W m^{-2} as an absolute minimum threshold for imaging and >500 W m^{-2} as a more typical minimum threshold. Finally, we determined the number of hours per day as a function of time of year and latitude when solar elevation would be suitable for avoiding sunglint: (1) 10-40°; and (2) 10-20°. The first case (10-40°) provided a window where solar elevation was high enough to minimize Fresnel reflectance but low enough to avoid sunglint on a flat surface for a down-looking sensor with a FOV of 80°. The second case (10-20°) provided an even more restricted window, where sunglint on rippled surfaces would likely be absent.

3. Results

3.1. Light-Dependent Constraints on the Optimal Imaging Window

The UAV surveys (N = 26) showed a variety of phenomena that hindered the ability to detect the riverbed, including reflection of the overlying cloud layer, the presence of sunglint, and the presence of shadow. For all imagery acquired under overcast skies (N = 7), riverbeds were either barely visible or not visible due to reflection of clouds off the water surface (e.g. Figure 3a, left panel). In contrast, for imagery acquired under cloud-free conditions (N = 16), riverbed detail was more apparent (e.g. Figure 3a, right panel). Estimated irradiant intensities at the time of imaging ranged from <100 to >500 W m^{-2}. The riverbed was visible even at the lowest estimated irradiant intensity (70 W m^{-2}), but was comparatively dark. From this, we inferred that an irradiant intensity of ca. 100 W m^{-2} would be an absolute minimum threshold, but that intensities in the vicinity of ca. 500 W m^{-2} were more favorable in terms of riverbed imaging. Imagery acquired under cloud-free conditions was susceptible to sunglint and shadow. When present, sunglint was apparent as specks on the ridges of ripples that obscured the underlying riverbed (Figure 3b, left panel); the same riverbed was visible through these ripples when sunglint was absent (Figure 3b, right panel). Sunglint was more prevalent in imagery acquired under high solar elevation (median solar elevation = 38.9°, range = 19.2 – 46.3°, N = 13); sunglint was absent under low solar elevation (median solar elevation = 15.1°, range = 12.5 – 21.1° , N = 3). In all imagery taken under cloud-free conditions, shadows were present when there was V-shaped valley-type topography and/or riparian vegetation dominated by trees (N = 12). Shadows in imagery of the Leirelva (N = 4) were largely absent due to a gentler cross-valley profile and fewer trees along the riverbank. Shadow prevalence was greater when the solar azimuth was near perpendicular to the channel than when the solar azimuth was aligned with the channel. For example, the riverbed was almost completely obscured in Figure 3c (left panel) due to obstruction of direct sunlight by a steep valley surrounding the channel. The riverbed in Figure 3d (right panel) was

 doi:10.20944/preprints202506.0278.v1

more visible because the solar azimuth was aligned with the channel, although some shadows were caused by overhanging vegetation.

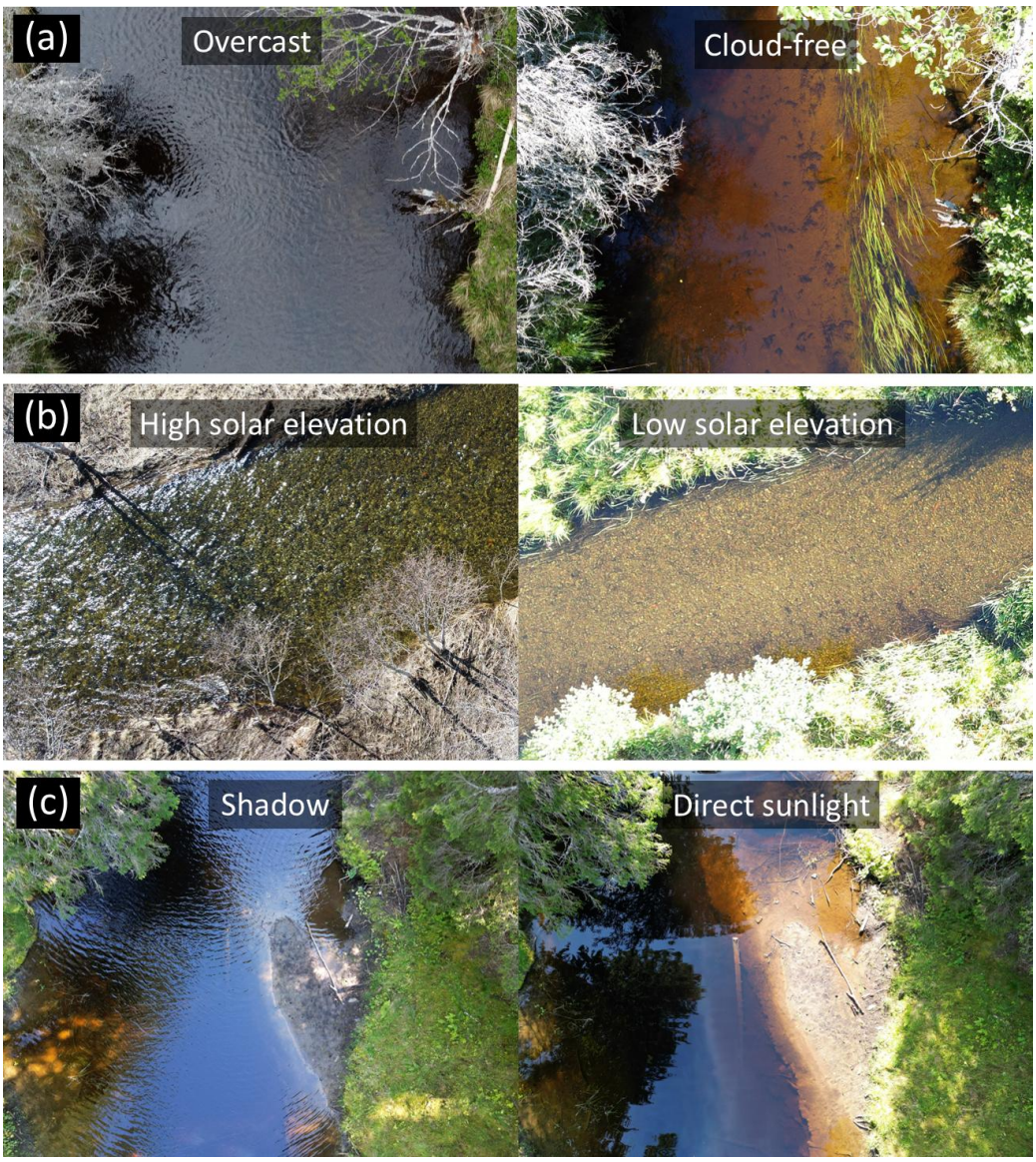

Figure 3. Effect of light environment on riverbed visibility: (a) cloud-cover (Borråselva); (b) solar elevation (Leirelva);. (c) shadow (Kobberdamsbekken).

The optimal imaging windows for the surveyed streams were constrained by: (1) cloud cover, which manifested as reflections off the water surface, masking the riverbed, (2) solar elevation, which affected irradiant intensity and sunglint; and (3) solar position, which affected shadow.

Cloud cover. All surveyed streams experienced high cloud cover throughout the year (Figure 4a). Mean annual cloud cover was ca. 75%, and consistently high throughout the year. Therefore, cloud cover will prevent successful imaging of the riverbed in the survey streams on an average of 3 out of 4 days throughout the year.

Solar elevation, irradiance and sunglint. The intra-diurnal pattern of solar elevation varied strongly throughout the year, with consequent effects on irradiance and sunglint. Irradiant intensities exceeded 600 W m^{-2} around noon in summer but were consistently less than 100 W m^{-2} throughout winter (Figure 4b). Irradiant intensity alone would be enough to restrict the imaging window to exclude winter months. Conversely, the propensity to sunglint during the high summertime solar elevations restricted the diurnal imaging window more during summer months. Solar elevations likely to lead to sunglint on a flat surface at 63°N (solar elevation >40° for a sensor FOV >80o) occurred

 doi:10.20944/preprints202506.0278.v1

for a 4 h period around noon in June-July; solar elevations likely to lead to sunglint on a rippled surface (solar elevation >20°) extended this period into early morning and late afternoon; for instance, from ≈06:00 – 18:00 Hrs. in June and July. The requirement to avoid sunglint while ensuring a solar elevation high enough to avoid Fresnel reflectance would greatly limit the optimal imaging window, allowing for imaging during a period of ca. 1 h in the early morning or the late afternoon in June-July.

Solar position and shadow. The surveyed streams were subject to shadow, depending on how topography and riparian vegetation obstructed direct sunlight, in turn dependent upon solar position. All the streams were always partly shaded (Figure 4c). The percentage of time under direct sunlight varied according to time of day, time of year, and site. High solar elevations resulted in less shading, so more of the streams were under direct sunlight around noon and towards the summer equinox. For example, all streams were >55% under direct sunlight at noon on the summer solstice, but were <55% under direct sunlight at noon on the autumn equinox. The configuration of the stream with respect to the solar azimuth also affected the intra-diurnal pattern. Mølnelva, which was aligned on a more south-north heading than the other streams, had a higher proportion of the channel under direct sunlight than the other streams when the solar azimuth was in a more southerly position around noon. For all streams, however, the requirement to image under direct sunlight pushed the optimal imaging window towards noon and the summer months.

 doi:10.20944/preprints202506.0278.v1

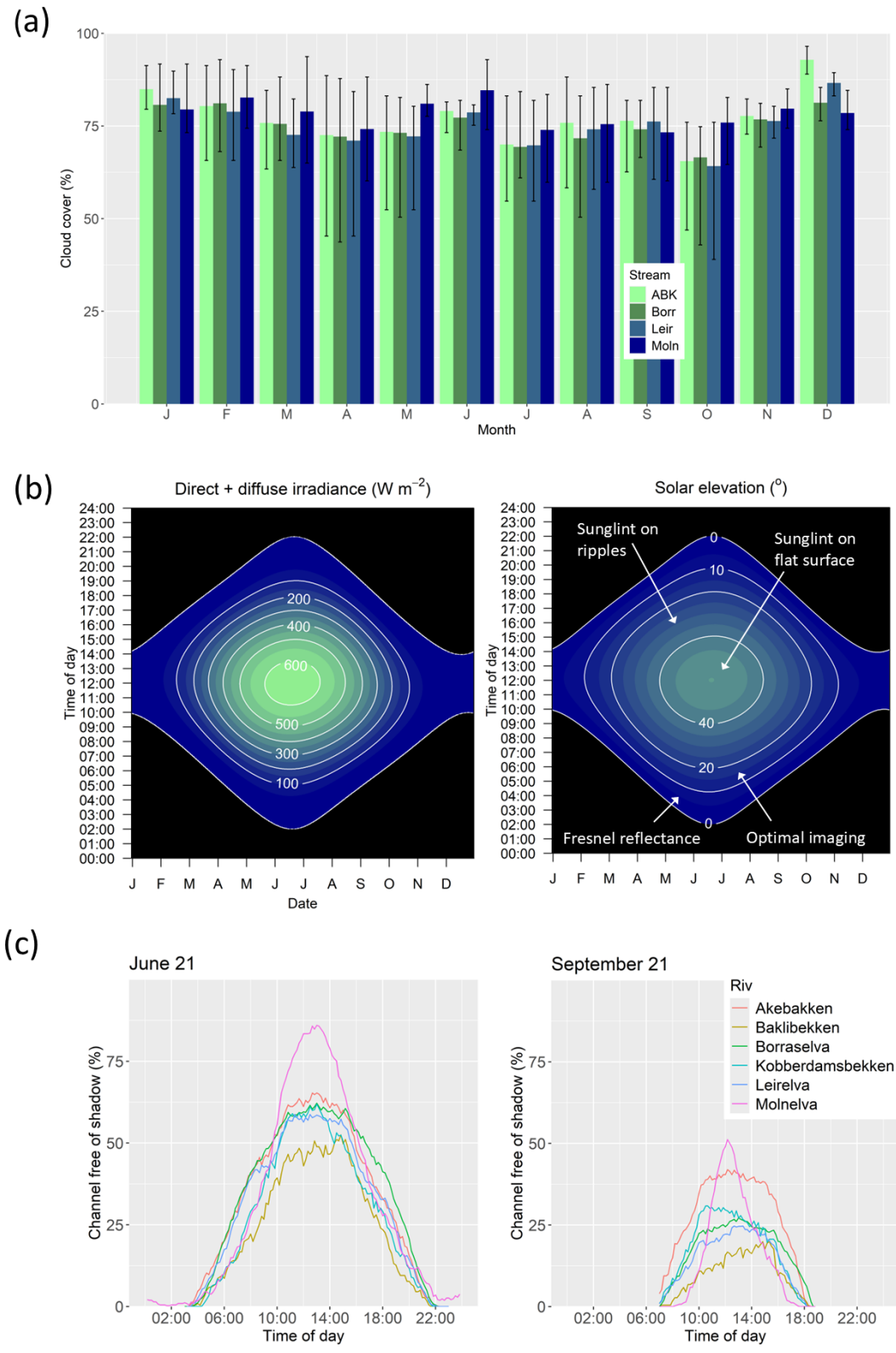

Figure 4. Constraints on the imaging window for survey streams: (a) cloud cover expressed as a mean monthly value (years 2016-2019): (b) solar irradiance and solar elevation (latitude = 63 °N); (c) percentage of stream channel under direct sunlight. In (a) cloud cover was obtained through the Cloud Fraction dataset of the NASA Earth Observations portal (https://neo.gsfc.nasa.gov/). In (b) and (c) solar irradiance and solar elevation was estimated using the R solrad library.

3.2. Regional Patterns of the Optimal Imaging Window Across Europe

 doi:10.20944/preprints202506.0278.v1

Generalizing our findings across Europe, we found large-scale, regional differences in constraints on the optimal imaging window that were related to (1) geographical differences in cloud cover and (2) latitudinal differences in solar elevation and therefore irradiant intensity and propensity to sunglint.

Cloud cover. Regional and intra-annual patterns in cloud cover existed across Europe, greatly restricting the number of days when a stream can be imaged in more northerly latitudes and in winter (Figure 5a). Year-round, the number of cloud free-days ranged from >200 in southern latitudes (e.g. Portugal to Greece) to <90 in the northern-western maritime coast of Europe (e.g. Ireland, UK and Norway). The number of cloud free days was generally greater in summer than winter, particularly in more southern locations. Therefore, cloud cover will not be a major limitation to UAV remote sensing of the riverbed in southern Europe during summer, but will pose a limitation at higher latitudes.

Solar elevation, irradiance, and sunglint. Latitudinal patterns in solar elevation affected intra-diurnal and intra-annual patterns of irradiance (Figure 5b). When assigning a low limit for a sufficient irradiant intensity for riverbed imaging (>100 W m^{-2}), a strong latitudinal gradient in the optimal imaging window existed in winter, from >6 h per day (latitude <40°N) to <1 h per day (latitude >54°N). However, with a higher irradiant intensity limit (>500 W m-2), imaging would not be possible regardless of latitude. Higher solar elevations and higher irradiant intensities during summer led to longer imaging windows per day than in winter. With a lower irradiant intensity threshold (>100 W m^{-2}), summertime imaging windows were longer in northern (> 14 h per day) than southern latitudes (< 12 h). With a higher threshold (>500 W m^{-2}), this gradient was reversed such that there was a longer imaging window in southern (>7 h per day) than in northern latitudes (<4 h). Latitudinal patterns in solar elevation also affected the propensity for sunglint, both on flat surfaces (occurring at solar elevations ca. >40° for a sensor with an 80° FOV) and on ripples (occurring at solar elevations at ca. >20°). This led to consequent latitudinal patterns in the optimal imaging window for avoiding sunglint (Figure 5c). Higher solar elevations in southern latitudes reduced daily optimal imaging windows to <6 h (avoiding persistent sunglint on flat surfaces while ensuring a solar elevation of >10° to avoid Fresnel reflectance) and <2 h (when avoiding sunglint on rippled surfaces). Lower solar elevations at higher solar latitudes allowed for a longer optimal imaging window during summertime: >9 h when avoiding sunglint on flat surfaces, and >3 h when avoiding sunglint on rippled surfaces.

 doi:10.20944/preprints202506.0278.v1

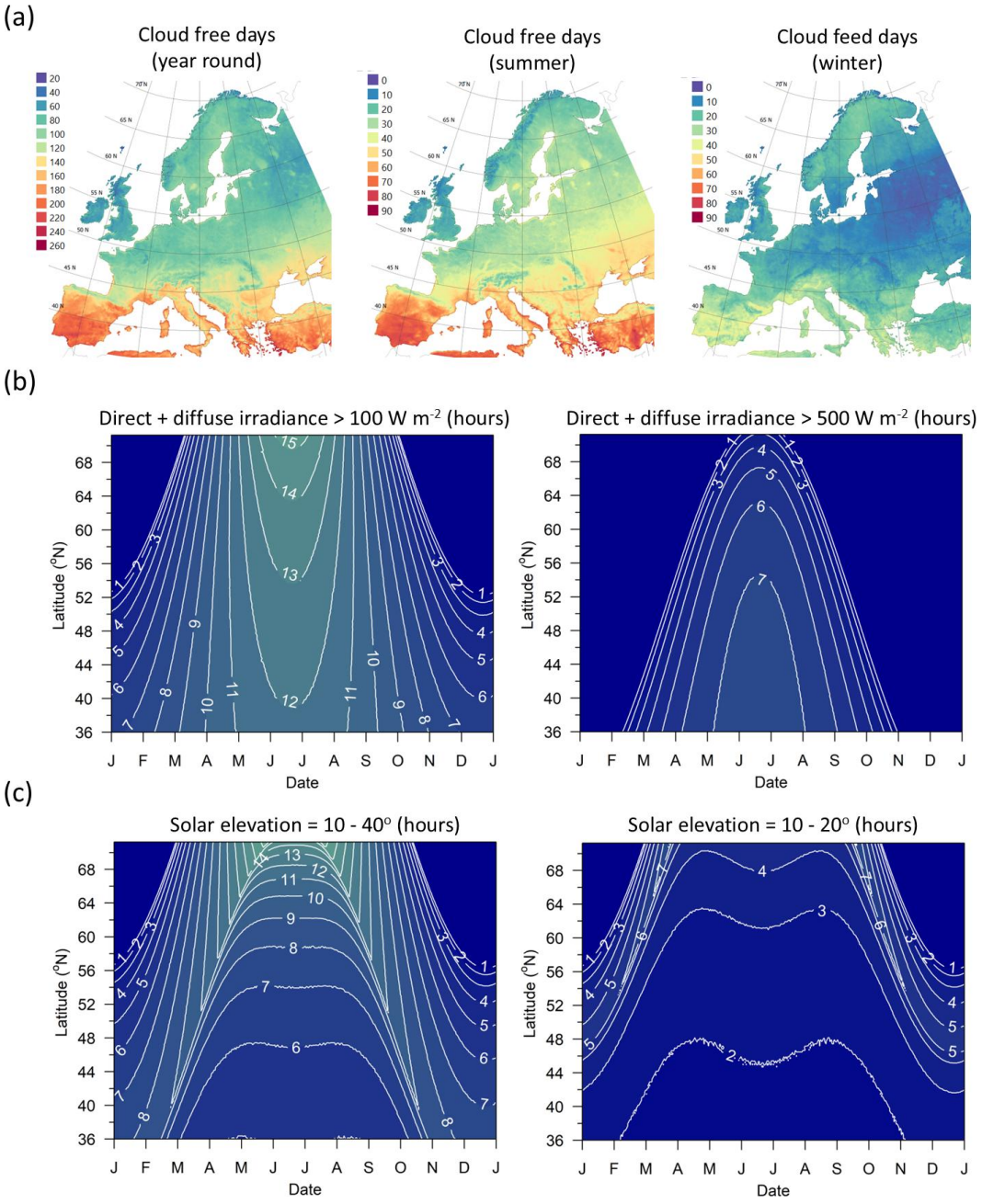

Figure 5. Optimal window length for UAV imaging across Europe: (a) cloud free days; (b) hours per day with solar irradiance >100 and >500 W m^{-2}; (c) hours per day when solar elevation is 10-40° and 10-20°. See Figure 4 for data sources.

4. Discussion

Effective optical remote sensing of the riverbed in small, tree-lined streams is difficult due to the requirement to obtain a suitable light environment. Using UAV surveys conducted under a range of light conditions, we found imagery is particularly susceptible to reflection of the overlying cloud layer at the water surface, and the presence of sunglint and shadow. We calculated that avoiding adverse light conditions would greatly limit the optimal imaging window, although the manner in which this restriction occurred would vary both regionally across Europe and according to local site characteristics. In the following sections we discuss constraints on the optimal window for surveying the riverbed in small, tree-lined streams. We then discuss the potential for expanding the optimal imaging window via careful image acquisition and image processing. Building on this, we present a protocol for optimal imaging that takes the light environment into account.

 doi:10.20944/preprints202506.0278.v1

4.1. Constraints on the Optimal Imaging Window

The optimal window for imaging the riverbed is dependent on regional and local variation in a range of factors affecting the light environment. Based on regional changes in cloud cover and solar elevation, European rivers can be placed in two classes: northern and southern.

Northern European rivers (e.g. latitudes >55°N) are characterized by high cloud cover throughout the year, such that cloud-free conditions for imaging only occur on ca. 25-30% of days within the year. Low solar elevations in winter lead to short-day lengths, and to low irradiant intensities even at noon. Thus, at northern latitudes, the optimal imaging window may be constrained within the year to exclude winter months. Conversely, the optimal imaging window within a day during summer months will be long due to the long day length. Although the generally low solar elevations encountered in northern latitudes lead to low irradiant intensity, they make the river surface less prone to sunglint, so it may not be necessary to interrupt imaging around noon.

Southern European rivers (e.g. latitudes <55°N) are characterized by less cloud cover throughout the year, such that cloud-free conditions for imaging exist on more than ca. two-thirds of days throughout the year. Conditions are cloudier in winter than summer, but imaging is still possible in winter on ca. one third of days. The less variable day length throughout the year does not greatly restrict the daytime imaging window in winter. However, higher solar elevations make water surfaces more prone to sunglint so the optimal imaging window within the day during summer may be greatly restricted. There is, however, the potential to expand this window with careful image acquisition and processing (see Section 4.2).

Optimal windows will further be reduced by the presence of shadows. This restriction is much more locally dependent than either the requirements of cloud-free conditions or optimal solar elevations, and will depend on both topography and riparian vegetation, both of which will vary locally. For example, north-south aligned rivers will be less affected by shadow than east-west aligned rivers when imaging around noon. However, for a given alignment, topography and vegetation cover, northern European rivers will be more affected than southern European rivers due to the generally lower solar elevations in northern latitudes.

4.2. Expanding the Optimal Imaging Window

Low irradiant intensities are a particular problem for imaging rivers in northern locations, particularly when imaging away from the summer solstice, because riverbed imagery will be dark and relatively noisy. The imaging window can be expanded to include darker ambient light conditions via image post-processing: for example, through contrast enhancement, and removal of noise using bilateral filters [21].

Sunglint is a particular problem for southern locations. Avoiding sunglint may reduce the daily imaging window in summer to only a few hours in the early morning and late afternoon. Adjustments to the surveying method or the processing of images may avoid or minimize the presence of sunglint and thus expand the optimal imaging window. With respect to a surveying method that minimizes the presence of sunglint in imagery, the sensor can be oriented away from the solar azimuth angle [22,23]. While this may reduce the presence of sunglint, the requirement to maintain a specific sensor orientation adds to surveying effort and may pose problems for creation of Structure-from-Motion orthophotos which require a range of view angles for effective creation. With respect to removal of sunglint present within imagery, a range of imaging approaches may be used. Single images may be cropped to remove sunglint and subsequently mosaiced [24]. Alternatively, ephemeral phenomena such as sunglint on ripples or wave lensing can be removed using a temporal filter applied to video imagery see [25]. Temporal filtering relies upon repeat imaging of an area (e.g. from a video acquired by a UAV), aligning frames so that each pixel among all frames refers to the same location, masking unwanted pixels (e.g. sunglint), and then constructing a single image from the retained pixels (see examples of removal of shallow water wave lensing in Figure 6). We have found, however, that this method requires careful control in surveying approach and is not always effective. Firstly, surveying effort is high, typically requiring surveying from a fixed

 doi:10.20944/preprints202506.0278.v1

position and ensuring the presence of a static land surface in the video to enable auto-alignment. Secondly, merged images may have artefacts. The use of information from multiple frames results in smoothing of riverbed detail due to imperfections in alignment and changes in geometric distortion between images, and it is therefore necessary to find the correct balance between removing surface-induced phenomena (sunglint, wave lensing) and over-smoothing of the riverbed detail. The most important limitation however is that the method will be less effective when the surface effects are less temporally variable (e.g. persistent sunglint on a flat surface).

Shadows pose a problem for both northern and southern locations. Imaging the river during a range of solar positions may allow for selective merging of shadow-free areas and increase the proportion of the river that is shadow-free in the constructed, composite image. Alternatively, shadow in individual images may be identified and filtered. There is ongoing research on shadow removal from UAV imagery [26,27]. This research has focused on terrestrial applications, but in principle, could be applied to water surfaces.

 doi:10.20944/preprints202506.0278.v1

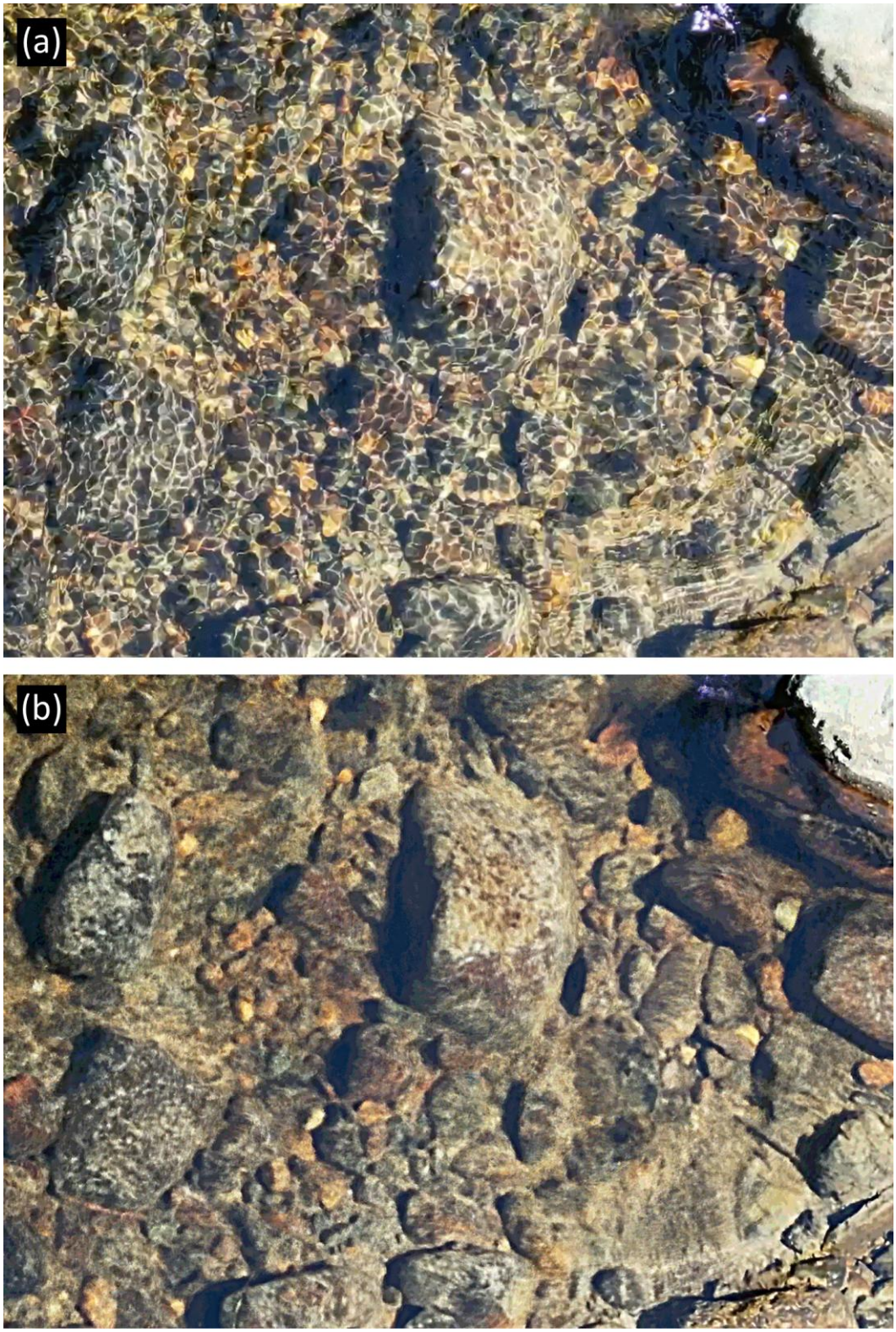

Figure 6. Example of removal of shallow water wave lensing: (a) a single frame from video acquired from Kobberdamsbekken; (b) a corresponding image constructed using a temporal filter applied to multiple frames (N = 25). Video frames were aligned using Photoshop. Aligned frames were then merged using a temporal filter, where the pixel for an x and y location in the merged image was selected from the pixel with the median value from all frames for that location. The constructed image has been sharpened using an unsharp mask (radius = 5 pixels, amount = 100%).

4.3. A Protocol for Optimal Riverbed Remote Sensing Using UAVs

 doi:10.20944/preprints202506.0278.v1

The advantage of UAV remote sensing with respect to imaging riverbeds in small tree-lined streams is that it offers greater flexibility over (1) *when* imaging is done (allowing selection of optimal light environments), (2) *how* the imaging is done (e.g. allowing selection of an optimal view angle with respect to the solar position), and (3) the *type of data* obtained (allowing for post-processing of collected imagery). This flexibility can be incorporated into a protocol so that UAV surveying can collect the best information possible. This should involve (1) identification of optimal windows for surveying prior to the survey attempt, (2) image acquisition under the best possible light conditions, and (3) post-processing of acquired imagery (Figure 7).

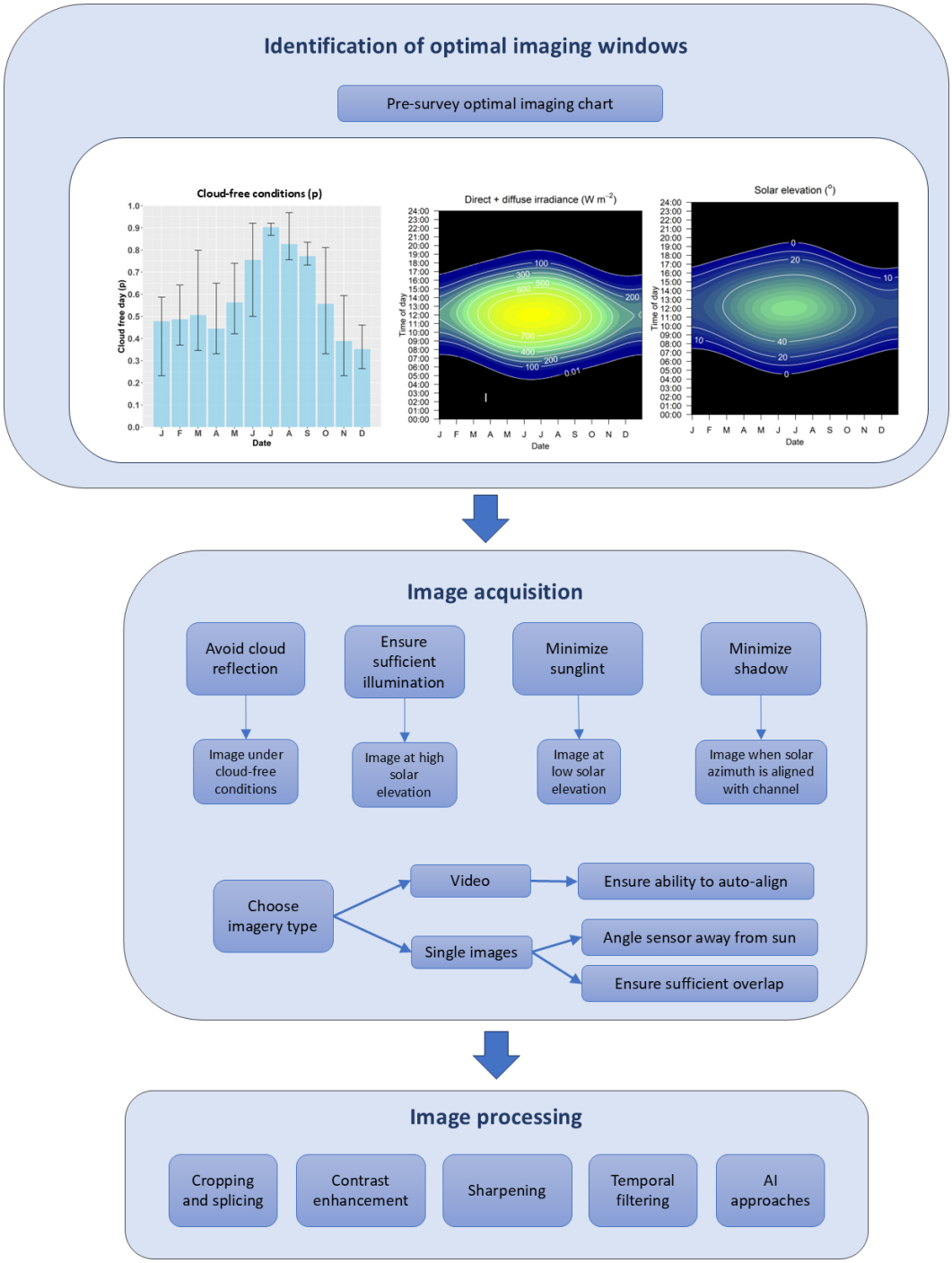

Figure 7. Recommended protocol for optimal remote sensing of riverbeds.

4.3.1. Identification of Optimal Imaging Windows

 doi:10.20944/preprints202506.0278.v1

Optimal imaging windows – both with respect to time of year and time of day – should be identified pre-survey to ensure the highest probability of success when the surveying is conducted. We recommend that a pre-survey optimal imaging chart is created for the survey location in question, describing historical patterns of cloud cover, solar elevation, and irradiance. If data on surface elevation around the site are available, we recommend that the shadow environment is estimated pre-survey for a range of solar positions. This approach enables gauging of the balance between conflicting light environment requirements: for instance, the requirement to maintain a high enough irradiant intensity to observe the riverbed while at the same time minimizing sunglint or shadow. In addition to identifying optimal imaging windows with respect to the light environment, it is also useful at this stage to identify the historic flow patterns within the stream which may impact riverbed visibility: for example, high discharges lead to more white water / foam on the surface and increased turbidity in the water column, affecting riverbed visibility.

Identification of optimal imaging windows can be used to (1) plan survey times for investigations that can be conducted irrespective of time of year and (2) assess the merits of using UAV remote sensing when there is a requirement to obtain information at a specific time of year. In the former case, many investigations can be conducted at any date within a year – for example, investigation of stable riverbed substrates. Here, it is prudent to select the optimal imaging time within the year to obtain the best data. In the latter case, some investigations may target time-specific phenomena. For example, salmon redd (i.e. spawning site) formation occurs in autumn, when solar elevations are low, and skies may be prone to cloud cover. Assessing the likelihood of successfully imaging the riverbed under such conditions can be used in determining whether UAV remote sensing is suitable and/or the resources that should be assigned to it.

4.3.2. Image Acquisition

After identification of optimal imaging windows, surveys can be planned so that imagery is obtained at a time when the likelihood of adverse light conditions are minimized. Based on site location, calculated solar positions can be used to ensure surveying occurs at sufficient irradiance levels, with minimal sunglint and shadow. This will influence the time of optimal imaging, both within the year (e.g. winter may be unsuitable for northern locations) and within the day (noon at summer may be unsuitable for southern locations). In the days leading up to surveying, short-term weather forecasts can be used to focus planned surveys towards days or hours when cloud-free conditions are expected.

The manner in which imagery is acquired should also take the light environment into account. If the solar elevation at imaging is likely to lead to sunglint, mitigation methods should be employed such as (1) off-nadir viewing, (2) ensuring that there is sufficient overlap between successive images to enable removal of sunglint-affected areas followed by image splicing, or (3) acquisition of video to allow for temporal filtering.

4.3.3. Image Processing

The extent to which image processing is required will depend on (1) the degree to which light-dependent phenomena (e.g. sunglint, shallow water wave lensing, ripples, shadows) that obscure the riverbed are present within the imagery and (2) the objectives of the investigation. Careful selection of the time of imaging may minimize the requirement for image processing, but some phenomena may inevitably be present (e.g. sunglint on ripples in southern rivers during summer). Depending on investigation objectives, it may not always be necessary to apply image processing. For example, a qualitative investigation of dominant substrate types may be possible even if there is patchy sunglint; in contrast, a quantitative measurement of the substrate size distribution may require processing to remove the sunglint. When required, a wide variety of image processing methods exist (see examples in Section 4.2) and researchers should plan for their use as part of the overall mission planning. This area is rapidly developing – in particular, machine learning approaches [28] – but researchers should take into account that they are dealing with a particularly complicated light environment, and that

 doi:10.20944/preprints202506.0278.v1

many of the techniques applied to wide, open low-land rivers may be less effective in small, more constrained streams.

5. Conclusions

The ability to use UAVs with mounted RGB cameras to survey the riverbed in small, tree-lined streams is dependent on the ambient light environment. Our analysis of multiple UAV surveys showed that imagery was subject to several phenomena – reflection of overlying clouds, sunglint, shadow – that reduced the ability to discern the riverbed. Avoiding suboptimal conditions reduces the available window for imaging, both within the year and within the day. The ambient light environment is region-specific. We therefore conclude that the main constraints on the optimal imaging window will differ between northern and southern rivers. Optimal imaging in northern rivers will be more constrained by avoidance of low irradiant intensities in winter; that in southern rivers will be more constrained by avoidance of solar elevations likely to lead to sunglint during the mid-part of the day. We recommend that surveying should take the ambient light environment into account. This should be investigated prior to surveying. Image acquisition should then target optimal imaging windows and be done in a manner that minimizes light environment problems or allows for subsequent removal through image processing.

Author Contributions: Conceptualization, RDH; methodology, RDH and MPG.; formal analysis, RDH; writing, RDH and MPG. All authors have read and agreed to the published version of the manuscript.

Funding: This research was funded by the Norwegian Institute for Nature Research (SATS 22-26 Hedger).

Data Availability Statement: Imagery and sample code are available on request.

Conflicts of Interest: The authors declare no conflicts of interest. The funders had no role in the design of the study; in the collection, analyses, or interpretation of data; in the writing of the manuscript; or in the decision to publish the results.

References

1. Papaioannou, G.; Markogianni, V.; Loukas, A.; Dimitriou, E. Remote Sensing Methodology for Roughness Estimation in Ungauged Streams for Different Hydraulic/Hydrodynamic Modeling Approaches. Water 2022, 14, doi:10.3390/w14071076.
2. Carbonneau, P.E.; Dugdale, S.J.; Breckon, T.P.; Dietrich, J.T.; Fonstad, M.A.; Miyamoto, H.; Woodget, A.S. Adopting deep learning methods for airborne RGB fluvial scene classification. Remote Sens. Environ. 2020, 251, doi:https://doi.org/10.1016/j.rse.2020.112107.
3. Giroux, C.; Grant, J.; Brown, C.J.; Barrell, J. Remote sensing of river habitat for salmon restoration. Frontiers in Remote Sensing 2022, 3:993575, doi:doi: 10.3389/frsen.2022.993575.
4. Singh, A.; Vyas, V. A Review on remote sensing application in river ecosystem evaluation. Spatial Information Research 2022, 30, 759–772, doi:doi.org/10.1007/s41324-022-00470-5fluxes.
5. Arif, M.S.M.; Gülch, E.; Tuhtan, J.A.; Thumser, P.; Haas, C. An investigation of image processing techniques for substrate classification based on dominant grain size using RGB images from UAV. Int. J. Remote Sens. 2016, 38, 1-23, doi:10.1080/01431161.2016.1249309.
6. Kislik, C.; Genzoli, L.; Lyons, A.; Kelly, M. Application of UAV Imagery to detect and quantify submerged filamentous algae and rooted macrophytes in a non-wadeable river. Remote Sens. 2020, 12, doi:10.3390/rs12203332.
7. Harrison, L.R.; Legleiter, C.J.; Overstreet, B.T.; Bell, T.; Hannon, J. Assessing the potential for spectrally based remote sensing of salmon spawning locations. River Research and Applications 2020, 36, 1618-1632, doi:10.1002/rra.3690.
8. Roncoroni, M.; Lane, S.N. A framework for using small Unmanned Aircraft Systems (sUASs) and SfM photogrammetry to detect salmonid redds. Ecol. Inform. 2019, 53, doi:10.1016/j.ecoinf.2019.100976.

 doi:10.20944/preprints202506.0278.v1

9. Hedger, R.D.; Gosselin, M.-P. Testing UAV surveying for mapping of fresh-water pearl mussel populations; NINA: 2022.
10. Forseth, T.; Fjeldstad, H.-P.; Gabrielsen, S.E.; Skår, B.; Lamberg, A.; Hedger, R.; Kvingedal, E.; Havn, T. Miljødesign Mandalselva – samlet tiltaksplan og oppsummering.; Norsk institutt for naturforskning: 2019.
11. Wang, M.X.; Wang, L.F.; Jiao, J.N.; Song, Q.J.; Ma, C.F.; Yang, S.; Ju, W.M.; Tian, L.Q.; Lu, Y.C. Sea surface Fresnel reflections difference driven de-glint algorithm for airborne optical images. Optics Letters 2024, 49, 4090-4093, doi:10.1364/ol.529026.
12. Dammeier, F.; Happle, G.; Rohrer, J. The contribution of water surface Fresnel reflection to BIPV yield. Solar Energy 2017, 155, 951-962, doi:10.1016/j.solener.2017.07.041.
13. Wilson, A.M.; Jetz, W. Remotely sensed high-resolution global cloud dynamics for predicting ecosystem and biodiversity distributions. Plos Biology 2016, 14, doi:10.1371/journal.pbio.1002415.
14. Garaba, S.P.; Zielinski, O. Methods in reducing surface reflected glint for shipborne above-water remote sensing. Journal of the European Optical Society-Rapid Publications 2013, 8, doi:10.2971/jeos.2013.13058.
15. Mount, R. Acquisition of through-water aerial survey images: Surface effects and the prediction of sun glitter and subsurface illumination. Photogrammetric Engineering and Remote Sensing 2005, 71, 1407-1415, doi:10.14358/pers.71.12.1407.
16. Ortega-Terol, D.; Hernandez-Lopez, D.; Ballesteros, R.; Gonzalez-Aguilera, D. Automatic Hotspot and Sun Glint Detection in UAV Multispectral Images. Sensors 2017, 17, doi:10.3390/s17102352.
17. Marcus, W.A.; Fonstad, M.A. Optical remote mapping of rivers at sub-meter resolutions and watershed extents. Earth Surface Processes and Landforms 2008, 33, 4-24, doi:10.1002/esp.1637.
18. Hedger, R.D.; Gosselin, M.-P. Automated fluvial hydromorphology mapping from airborne remote sensing. River Research and Applications 2023, 1-13, doi:DOI: 10.1002/rra.4186.
19. Veal, C.J.; Carmi, M.; Dishon, G.; Sharon, Y.; Michael, K.; Tchernov, D.; Hoegh-Guldberg, O.; Fine, M. Shallow-water wave lensing in coral reefs: a physical and biological case study. J. Exp. Biol. 2010, 213, 4304-4312, doi:10.1242/jeb.044941.
20. Seyednasrollah, B.; Kumar, M.; Link, T.E. On the role of vegetation density on net snow cover radiation at the forest floor. Journal of Geophysical Research-Atmospheres 2013, 118, 8359-8374, doi:10.1002/jgrd.50575.
21. Ansari, E.; Akhtar, M.N.; Abdullah, M.N.; Othman, W.; Abu Bakar, E.; Hawary, A.F.; Alhady, S.S.N. Image Processing of UAV Imagery for River Feature Recognition of Kerian River, Malaysia. Sustainability 2021, 13, doi:10.3390/su13179568.
22. Mobley, C.D. Estimation of the remote-sensing reflectance from above-surface measurements. Applied Optics 1999, 38, 7442-7455, doi:10.1364/ao.38.007442.
23. Slocum, R.; Wright, W.; Parrish, C.; Costa, B.; Sharr, M.; Battista, T. Guidelines for Bathymetric Mapping and Orthoimage Generation using sUAS and SfM, An Approach for Conducting Nearshore Coastal Mapping. ; 2019.
24. Gilvear, D.J.; Davids, C.; Tyler, A.N. The use of remotely sensed data to detect channel hydromorphology; River Tummel, Scotland. River Research and Applications 2004, 20, 795-811, doi:10.1002/rra.792.
25. Partama, I.; Kanno, A.; Ueda, M.; Akamatsu, Y.; Inui, R.; Sekine, M.; Yamamoto, K.; Imai, T.; Higuchi, T. Removal of water-surface reflection effects with a temporal minimum filter for UAV-based shallow-water photogrammetry. Earth Surface Processes and Landforms 2018, 43, 2673-2682, doi:10.1002/esp.4399.
26. Agarwal, A.; Kumar, S.; Singh, D. An Adaptive Technique to Detect and Remove Shadow from Drone Data. Journal of the Indian Society of Remote Sensing 2021, 49, 491-498, doi:10.1007/s12524-020-01227-z.

 doi:10.20944/preprints202506.0278.v1

27. Alvarado-Robles, G.; Solis-Munoz, F.J.; Garduno-Ramon, M.A.; Osornio-Rios, R.A.; Morales-Hernandez, L.A. A Novel Shadow Removal Method Based upon Color Transfer and Color Tuning in UAV Imaging. Applied Sciences-Basel 2021, 11, doi:10.3390/app112311494.
28. Ermilov, A.A.; Benko, G.; Baranya, S. Automated riverbed composition analysis using deep learning on underwater images. Earth Surface Dynamics 2023, 11, 1061-1095, doi:10.5194/esurf-11-1061-2023.